

Exploration of stable, mixed metal oxo clusters: a step towards atomically precise doping

Dietger Van den Eynden* and Ajmal Roshan Unniram Parambil†

Department of Chemistry, University of Basel, Mattenstrasse 24a, 4058 Basel, Switzerland

Metal oxo clusters are very interesting materials as they can be considered the smallest conceivable nanocrystal prototypes. In comparison with nanocrystals, they are atomically precise, meaning that they have a polydispersity of zero. Therefore, they are suitable materials as building blocks of complex structures. In an attempt to gain control on the doping levels of nanocrystals, one could envision the use of doped metal oxo clusters as seeds for the nanocrystals. Unfortunately, they have been scarcely studied. Here we study, computationally using Quantum Espresso, how stable these mixed clusters with zirconium (Zr), hafnium (Hf) and cerium (Ce) metals are, compared to the monometallic clusters. First, we optimized the calculation parameters and found that a 3x3x3 k-mesh is enough to obtain accurate results combined with an *ecutrho* of 50 and an *ecutwfc* of 350. Afterwards, we studied bimetallic mixed clusters (**ZrCe** and **HfCe**) and found that all of them are more stable compared to the monometallic cluster except **ZrCe5**, **HfCe5**. When mixing Zr and Hf, only the **Zr4Hf2**, **Zr3Hf3** mer and **ZrHf5** complex are more stable compared to the monometallic cluster. However, the differences are small. Finally, we studied the mixed clusters with all three metals inside and found that all mixed clusters are more stable compared to their monometallic counter parts.

I. INTRODUCTION

Group 4 metal oxo clusters (0.5 nm) are an interesting alternative for their bigger analogues, which are group 4 metal oxo nanocrystals (5 nm). They are atomically precise meaning that they exhibit a polydispersity of 0 and can be synthesized relatively easier by mixing a metal alkoxide with an excess carboxylic acid at room temperature.[1] Clusters under study consists of an octahedral core with 6 metal atoms on the edges and 8 oxygen atoms in the triangular planes in between the metal atoms. The core itself has a nearly identical structure to that of a cubic unit cell of bulk zirconium oxide. Their surface is capped with organic ligands, mainly short and rigid carboxylic acids.[2, 3] Therefore, these clusters can be regarded as hybrid objects, similar to nanocrystals since they consist of an inorganic core (providing physical properties) capped with an organic ligand and shell (providing chemical properties). On the other hand, the nanocrystals are usually synthesized at very high temperatures (>250°C) and exhibit a polydispersity of 5% in the best cases.[4–6] The clusters can be used as polymer fillers[7, 8], catalysts[9, 10], complex porous 3D-structures[11, 12], and photo UV resists.[13, 14] Moreover, they can be used as nucleation centers in nanocrystal synthesis enabling unprecedented size control.[15, 16] From this, one could envision the use of doped clusters as nucleation seeds as this would simultaneously allow for size control and dopant control. So far, the latter remains a challenge in the nanocrystal world. Though

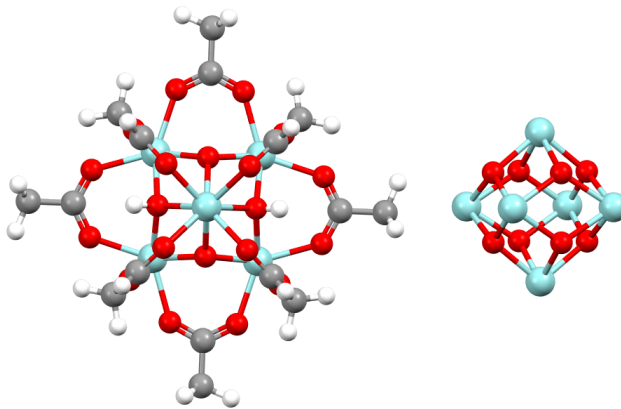


FIG. 1. Structure of metal oxo cluster ($M_6O_4(OH)_4(CH_3COO)_{12}$, where $M = Zr/Hf/Ce$) capped with acetate ligands. The M_6O_8 core is shown on the right. Cyan atoms represent either zirconium, hafnium or cerium; all other atoms follow conventional CPK coloring.

mono metallic clusters of zirconium, hafnium and cerium have been reported, the mixed metal clusters have been barely studied. In order to gain some insight, we hereby calculated bimetallic and trimetallic mixed metal clusters to discover which structures are viable options. This will give us a better insight as to which structures are theoretically plausible and can be exploited experimentally in laboratories.

II. BASIS SET OPTIMIZATION

In order to perform density functional theory calculations using quantum espresso, we have to optimize the basis set and other calculation parameters such as

* Department of Chemistry, University of Ghent, Krijgslaan 281, 9000 Ghent, Belgium; dietger.vandeneinden@unibas.ch

† Institute of Chemistry and Bioanalytics, School of Life Sciences, University of Applied Sciences and Arts Northwestern Switzerland, 4132 Muttenz, Switzerland; ajmal.roshan@unibas.ch

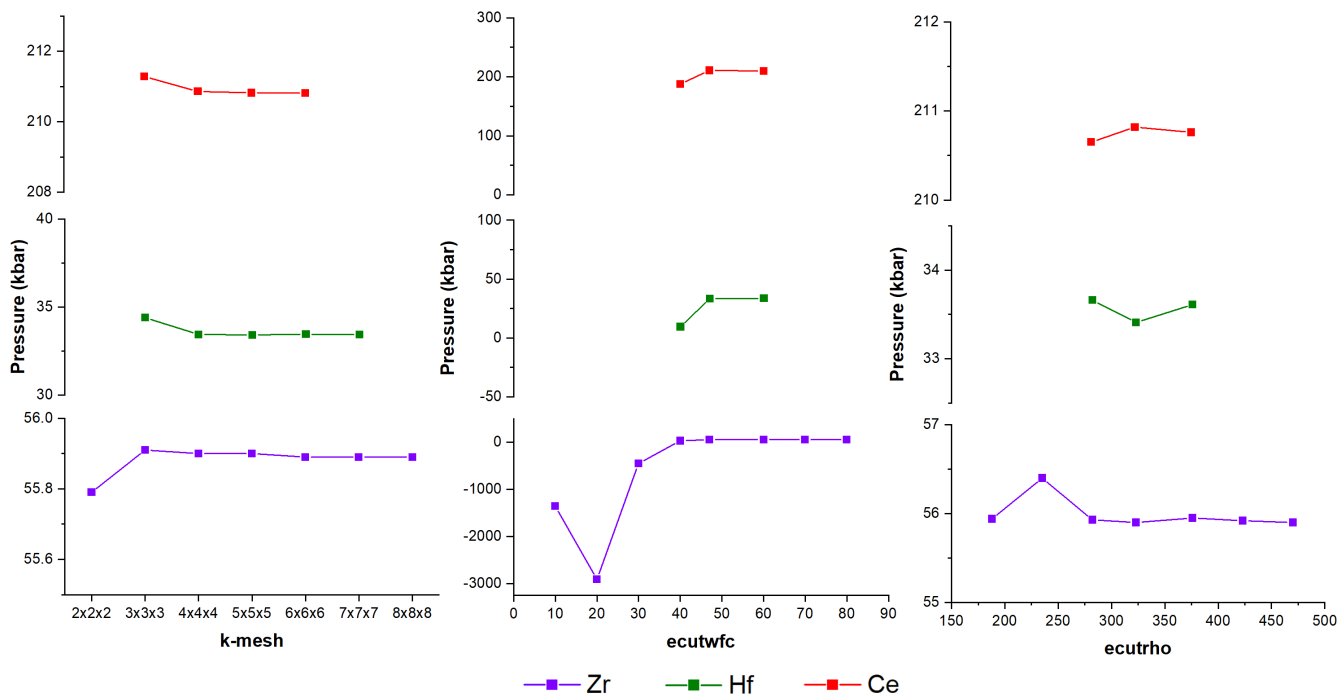


FIG. 2. k-mesh, ecutwfc and ecutrho optimization of zirconium, hafnium and cerium oxo clusters.

ecutrho and ecutwfc to obtain reliable results. For **Zr6** clusters, we started with the k-mesh optimization ranging from 1x1x1 to 8x8x8. Subsequently, the ecutwfc was changed from 10-80 in steps of 10 while keeping the ecutwfc/ecutrho ratio constant at 7. Finally, the ecutwfc/ecutrho ratio was varied from 4-10. The obtained parameters are plotted in figure 2. Once the optimized values were obtained, they were tested for both **Hf6** and **Ce6** clusters. Since the total energy is not a very sensitive unit to check the convergence, we tracked the pressure. The inorganic clusters are typically capped with organic ligands, therefore twelve acetate ligands per cluster were also added during the optimization/calculation. A typical cluster is displayed in figure 1.

A. Basis set optimization zirconium oxo clusters

From figure 2, it is clear that the pressure is stable (+- 1 kbar) from the 3x3x3 k-mesh onwards. Therefore, this value was chosen for further calculations. It is not surprising that a small k-mesh is sufficient since the unit cell of our system is relatively big which makes the first Brillouin zone small. For the ecutwfc optimization, the pressure is stable from 47 and above. The value 47 was obtained as the proposed ecutwfc in the basis set file. For convenience, we chose ecutwfc = 50 and continued further. The ratio between ecutrho and ecutwfc does not seem to have much influence on the pressure. However, since this would not drastically increase the calculation

time, we opted to go for a safe ratio of 7.

B. Basis set optimization hafnium oxo clusters

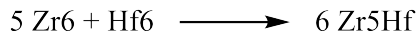
Since the parameters were already optimized for **Zr6** clusters, we used only a few calculations to show that these parameters are also valid for **Hf6** clusters. The k-mesh was varied between 3x3x3 and 7x7x7. ecutwfc was varied between 40-60 in steps of 10 and finally, the ratio between ecutrho and ecutwfc was varied between 6-8. It is clear from figure 2 that the k-mesh and the ecutrho/ecutwfc ratio do not show a great effect on the pressure. The ecutwfc on the other hand, only seems to give stable results from 47 or higher. Therefore, we concluded that the parameters found for **Zr6** clusters are also valid for **Hf6** clusters.

C. Basis set optimization cerium oxo clusters

For **Ce6** clusters, the same smaller optimization parameters were calculated as for **Hf6** clusters. The conclusions are exactly the same as can be seen in figure 2. Thus, the optimized parameters for **Zr6** cluster can be used here as well.

III. BIMETALLIC CLUSTERS

Once the optimized parameters were obtained, mixed metal clusters were calculated. Three different types of mixed clusters were calculated **Zr-Hf** clusters, **Zr-Ce** clusters and **Hf-Ce** clusters, respectively. In order to obtain the delta H for the formation reaction of mixed clusters compared to the formation of pure metal clusters, the balanced chemical equations were taken into consideration. (e.g. for **Zr5Hf** clusters in figure 3).



$$\Delta H = [6 * E_{\text{Zr5Hf}}] - [(5 * E_{\text{Zr6}}) + (E_{\text{Hf6}})]$$

FIG. 3. Schematic that shows how the values for delta H were obtained from the balanced chemical equation (top) and the calculation (bottom). In order to obtain the formation energy for one cluster, the calculated value was divided by 6.

If the value for delta H was negative, the mixed cluster is more stable compared to the monometallic clusters. For the bimetallic clusters, there are several options for the cluster to position both metals. For the M1xM2y clusters with x=1 and y=5, only 1 conformation is distinguishable since the other positions are equal due to the symmetry of the octaeder. When x=4 and y=2 or vice versa the metals can be arranged in either a cis or a trans configuration. Finally, when x=y=3 again, 2 different structures can be obtained, which are labelled fac and mer.

A. Mixed zirconium-hafnium clusters

Since Zr and Hf are so similar, the difference for different cluster compositions was expected to be smaller (Table I). The ionic radii of zirconium and hafnium in clusters are nearly the same (Zr4+ = 78 ppm, Hf4+ = 79 ppm). This appears in the delta H difference of **Zr-Hf** clusters compared to the **Zr-Ce** or **Hf-Ce** clusters. For x=4 and y=2, the cis conformation is more stable for **Zr4Hf2** clusters, and the trans configuration is more stable for the **Zr2Hf4** clusters. However, the difference is relatively small - 0.14 kJ/mol for both complexes. For the x=y=3 configuration, the mer configuration is more stable by 1.4 kJ/mol (Figure 4A). By looking at the Boltzmann equation, one can calculate the ratio between 2 or more stable conformations based on the energy difference.[17] Therefore, based on the energy difference of 0.14 kJ/mol, a mixture of 51% cis **Zr4Hf2** and 49% **Zr4Hf2** trans is expected. Since the **Zr2Hf4** and the **Zr3Hf3** fac clusters are less stable compared to the monometallic cluster, this calculation would be obsolete.

TABLE I. Enthalpy of formation of mixed zirconium-hafnium clusters.

ZrxHfy	Isomer	ΔH (kJ/mol)
Zr6	-	0
Zr5Hf	-	1.15
Zr4Hf2	cis	-0.90
Zr4Hf2	trans	-0.76
Zr3Hf3	fac	0.11
Zr4Hf2	mer	-1.30
Zr2Hf4	cis	1.16
Zr2Hf4	trans	1.30
ZrHf5	-	-0.90
Hf6	-	0

B. Mixed zirconium-cerium clusters

Interestingly, all mixed metal clusters are more stable compared to the monometallic clusters except for the **ZrCe5** cluster, which has a positive delta H (4.1 kJ/mol) (Table II & Figure 4B). For x=4 and y=2 conformers, the trans complex is more stable in both cases, by 10.4 and 18.5 kJ/mol for the **Zr4Ce2** and **Zr2Ce4** clusters, respectively. For the x=y=3 mixed clusters, the fac conformer is more stable. Since the energy differences are bigger for the Zr-Ce mixed clusters, the relative ratios show that most of the complexes will be in the most stable form. The **Zr4Ce2** cluster is expected to be 98.5% in its trans conformation. The **Zr3Ce3** cluster is expected to be 96.3% in its fac conformation. Finally, the **Zr2Ce4** clusters will almost exclusively be in their trans conformation (99.9%).

TABLE II. Enthalpy of formation of mixed zirconium-cerium clusters.

ZrxCey	Isomer	ΔH (kJ/mol)
Zr6	-	0
Zr5Ce	-	-8.42
Zr4Ce2	cis	-5.84
Zr4Ce2	trans	-16.22
Zr3Ce3	fac	-15.27
Zr4Ce2	mer	-7.19
Zr2Ce4	cis	-19.65
Zr2Ce4	trans	-38.14
ZrCe5	-	0.70
Ce6	-	0

C. Mixed hafnium-cerium clusters

Again, all mixed metal clusters are more stable compared to monometallic clusters except the **HfCe5** cluster, which has a positive delta H (3 kJ/mol) (Table III & Figure 4C). This shows that most of these mixed metal cluster formations are thermodynamically favourable. Furthermore, when comparing the cis and trans conforma-

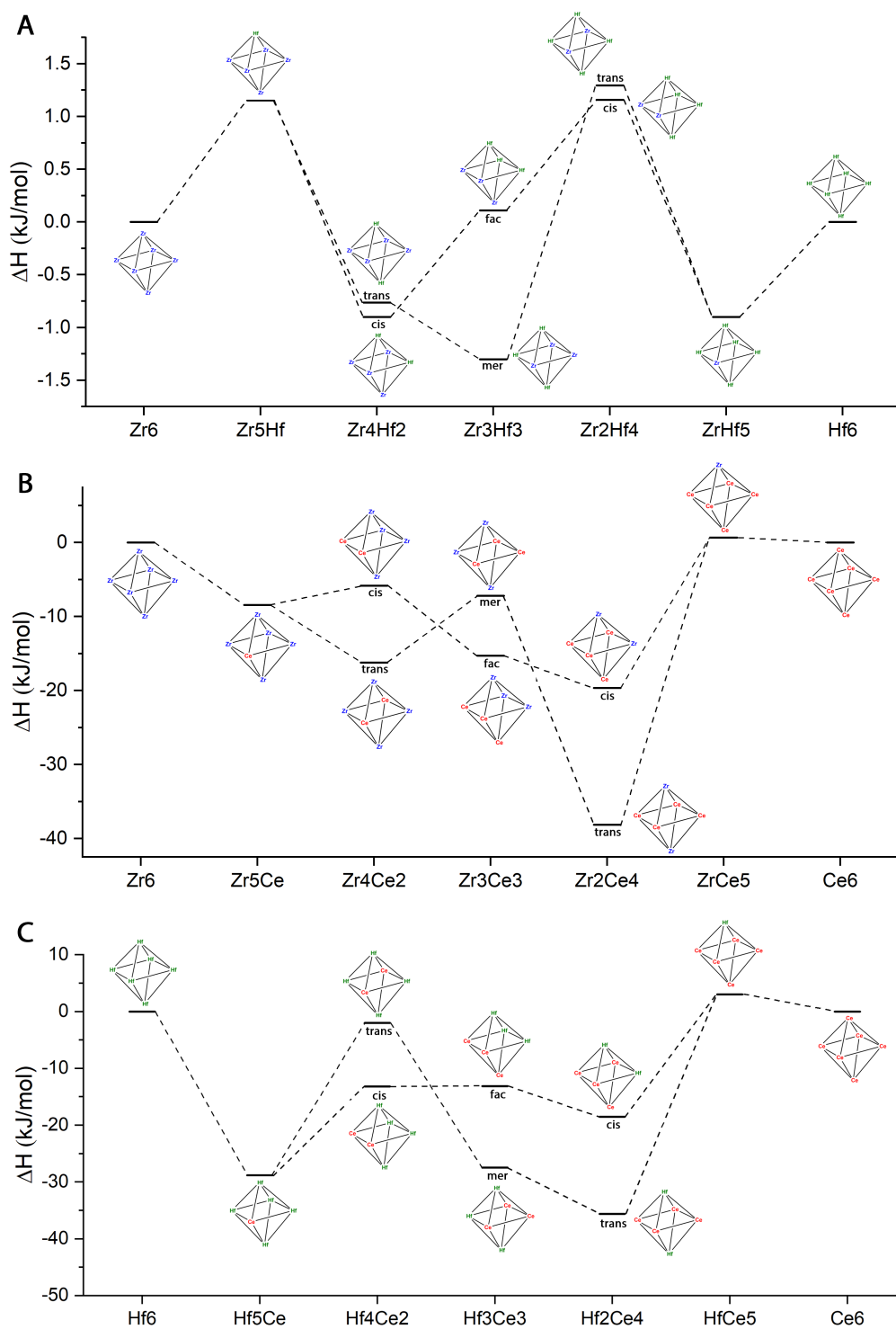


FIG. 4. Energy level diagram of (A) zirconium-hafnium, (B) zirconium-cerium and (C) hafnium-cerium mixed bimetallic oxo clusters. The corresponding structure of octahedra is also provided

tion of the $x=4$ and $y=2$, some interesting differences are observed. For the **Hf₄Ce₂** cluster, the trans conformer is more stable by 11 kJ/mol. On the contrary, for the **Hf₂Ce₄** cluster, the cis conformer is more stable (17 kJ/mol). For the $x=y=3$ case, the mer conformer is

more stable. Even though Zr and Hf are considered twin metals due to the lanthanide contraction, they exhibit different reactivity when mixed clusters with cerium are formed. In **ZrCe** clusters, it is twice the trans configuration which is more stable, whereas in **HfCe** clusters,

it is once the trans and once the cis configuration that is more stable. Also for the $x=y=3$ state, the fac conformer is more stable for **Zr-Ce** clusters in contrast to the mer conformation for **Hf-Ce** clusters. For the **Hf-Ce** clusters, the difference is even larger compared to the **Zr-Ce** clusters. This results in the main fraction of the conformations being in the most stable form (>99%).

TABLE III. Enthalpy of formation of mixed hafnium-cerium clusters.

HfxCey	Isomer	ΔH (kJ/mol)
Hf6	-	0
Hf5Ce	-	-28.86
Hf4Ce2	cis	-13.21
Hf4Ce2	trans	-1.99
Hf3Ce3	fac	-13.14
Hf4Ce2	mer	-27.46
Hf2Ce4	cis	-18.55
Hf2Ce4	trans	-35.62
HfCe5	-	3.00
Ce6	-	0

IV. TRIMETALLIC CLUSTERS

As the number of metals increases, the number of possible isomers increases (Figure 5A). The possible ratios of x,y and z are 2:2:2, 1:1:4 and 1:2:3. Five isomeric structures are possible for **Zr2Hf2Ce2** clusters, namely cis, trans, Zr-trans, Hf-trans and Ce-trans. When metals hold the ratio 1:1:4, six different structures need to be considered. Interestingly, when the ratio of metals is 1:2:3, eighteen isomers can be obtained. Due to time constraints, 3 of the 29 calculations, namely **ZrHf2Ce3** complex 3, **ZrHf3Ce2** complex 3, and **Zr3HfCe2** complex 3 couldn't be included since they didn't converge even after 200 iterations. The enthalpy of formation for every structure is negative, indicating all the trimetallic zirconium-hafnium-cerium mixed oxo clusters are stable compared to their corresponding monometallic ones (Table IV & Figure 5B). It is quite surprising to observe that the enthalpy of formation of isomers having exactly one cerium atom has similar energy. As the number of cerium metal raised to two or three, the energy differences between isomers are quite high. Moreover, for the 1:2:3 ratio complexes they all have at least 1 isomer which has a formation enthalpy of approximately -30 kJ/mol. This indicates that it might be very challenging to obtain a single isomer with 1 specific ratio experimentally.

V. CONCLUSION

We were able to successfully optimize the basis set parameters for all three different metal complexes. By changing the k-mesh, $ecutwfc$ and $ecutrho$, we found that

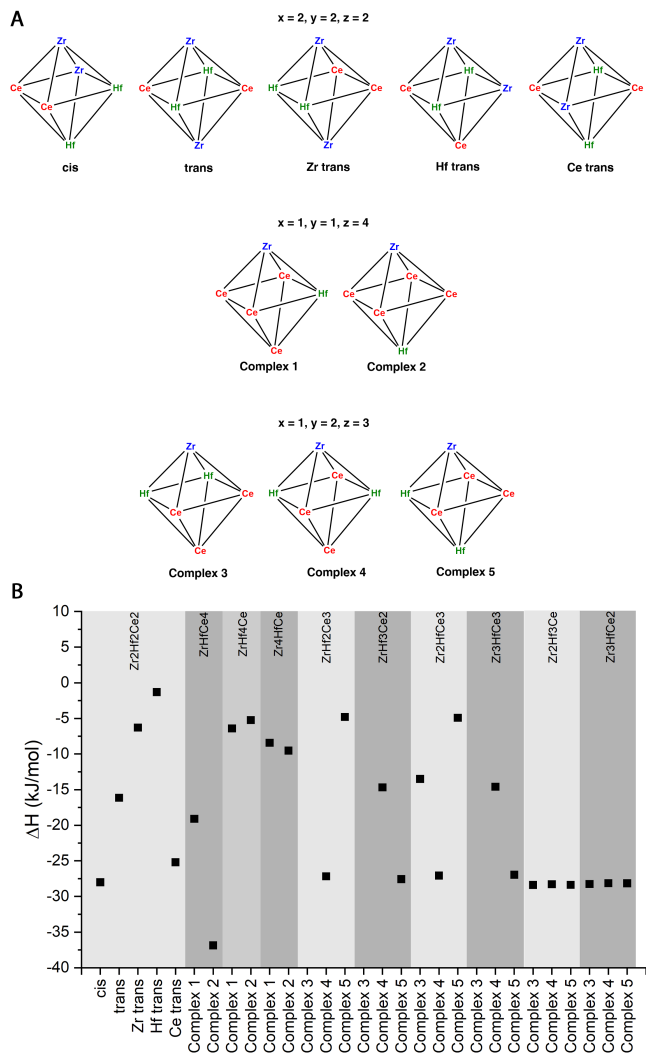


FIG. 5. (A) Possible structures of zirconium-hafnium-cerium trimetallic clusters. For 2:2:2, all possible structures are shown. For 1:1:4, four more structures are possible by changing the relative ratio of the metals. Similarly, for 1:2:3, changing the ratio results in 15 more structures. (B) Energy levels of Zr-Hf-Ce trimetallic clusters.

stable values for the pressure were obtained when the k-mesh is $3 \times 3 \times 3$, $ecutwfc$ is 50 and the $ecutrho$ is 350. The ratio between $ecutwfc$ and $ecutrho$ was kept at 7 even though stable results were obtained with lower ratios since this does not affect computational time drastically. Afterwards, several bimetallic and trimetallic cluster complexes were calculated with these optimized parameters. For the bimetallic clusters, it was clear that the differences for **ZrHf** clusters were smaller as compared to the mixed **ZrCe** and **HfCe** clusters. This is due to the similar ionic radii, which are 0.84 pm for Zr and 0.83 pm for Hf. Therefore, when cerium (ionic radius is 97 pm) is mixed with another metal in the cluster, the lattice mismatch might have a bigger effect on certain isomers resulting in a bigger energy difference. For **ZrHf**

TABLE IV. Enthalpy of formation of mixed zirconium-hafnium-cerium clusters.

ZrxHfyCez	Isomer	ΔH (kJ/mol)
Zr2Hf2Ce2	cis	-28.00
Zr2Hf2Ce2	trans	-16.15
Zr2Hf2Ce2	Zr trans	-6.30
Zr2Hf2Ce2	Hf trans	-1.31
Zr2Hf2Ce2	Ce trans	-25.20
ZrHfCe4	complex 1	-19.10
ZrHfCe4	complex 2	-36.87
ZrHf4Ce	complex 1	-6.42
ZrHf4Ce	complex 2	-5.23
Zr4HfCe	complex 1	-8.43
Zr4HfCe	complex 2	-9.52
ZrHf2Ce3	complex 3	
ZrHf2Ce3	complex 4	-27.17
ZrHf2Ce3	complex 5	-4.79
ZrHf3Ce2	complex 3	
ZrHf3Ce2	complex 4	-14.68
ZrHf3Ce2	complex 5	-27.56
Zr2HfCe3	complex 3	-13.51
Zr2HfCe3	complex 4	-27.07
Zr2HfCe3	complex 5	-4.91
Zr3HfCe2	complex 3	
Zr3HfCe2	complex 4	-14.60
Zr3HfCe2	complex 5	-26.96
Zr2Hf3Ce	complex 3	-28.39
Zr2Hf3Ce	complex 4	-28.28
Zr2Hf3Ce	complex 5	-28.37
Zr3HfCe2	complex 3	-28.26
Zr3HfCe2	complex 4	-28.15
Zr3HfCe2	complex 5	-28.16

clusters, the cis isomers seem to be more stable compared to the trans isomers. However, the energy difference is relatively small. A second observation is that both the **Zr5Hf** and the **Zr2H4** clusters do not seem to be viable options as they do not exhibit a negative formation enthalpy. When cerium is added, we couldn't elucidate a trend on the stability of isomers. An interesting observation that can be exploited experimentally while doping is that for both the **ZrCe** and the **HfCe** clusters, all but one isomer have a negative formation enthalpy indicating that they are viable complexes. The **ZrCe5** and the **HfCe5** clusters on the other hand do not seem to be feasible clusters based on their positive formation enthalpy. Interestingly, when all 3 metals were mixed into a cluster, all combinations gave negative formation enthalpies indicating that they can be formed. However, a clear trend could not be observed and should be studied in more detail. Remarkably, the clusters with a 1:2:3 ratio all have

at least 1 isomer, which seems very stable compared to the monometallic clusters (approx. -30 kJ/mol). This indicates that it will be challenging to obtain one single isomer of a specific metal ratio experimentally since most of them seem very stable compounds. Finally, it has to be noted that while these observations are interesting, more experimental data is needed. We show here which isomers are thermodynamically favourable but this does not mean that they are kinetically feasible, as not all of the metal precursors will react with the same speed. Additionally, all calculations are performed at 0 K, which is also a big difference between the theoretical and experimental approaches. Despite these considerations, the calculations gave us a first insight as to which isomers can be formed. The molar ratios for experimental cluster synthesis can be easily elucidated from the energy profiles, and the hunt to mixed metal oxo clusters which can be used as nanocrystal templates is on.

ACKNOWLEDGMENTS

The authors would like to thank Prof. Dr S. Cottelier for his support and constructive feedback during this project and for allowing us to perform a custom project. The authors would like to thank the university of Basel for the computational support.

Appendix A: Computational calculations

The projector augmented wave (PAW) approach was applied in combination with the Perdew-Burke-Ernzerhof (PBE) approximation for the exchange-correlation functional during the density functional theory calculations using QuantumESPRESSO.[18–21] A 3x3x3 k-mesh was used in all calculations together with an *ecutwfc* of 50 and *ecutrho* of 350. We used the following pseudo potentials obtained from <http://www.quantum-espresso.org>:

TABLE V. Enthalpy of formation of mixed hafnium-cerium clusters.

Atom	Pseudo potential
Zr	Zr.pbe-spn-kjpaw _p sl.1.0.0.U ^{PP} F
Hf	Hf.pbe-spn-kjpaw _p sl.1.0.0.U ^{PP} F
Ce	Ce.pbe-spdn-kjpaw _p sl.1.0.0.U ^{PP} F
O	O.pbe-n-kjpaw _p sl.1.0.0.U ^{PP} F
C	C.pbe-n-kjpaw _p sl.1.0.0.U ^{PP} F
H	H.pbe-kjpaw _p sl.1.0.0.U ^{PP} F

[1] D. Van den Eynden, R. Pokratath, J. P. Mathew, E. Goossens, K. De Buysser, and J. De Roo, Fatty acid capped, metal oxo clusters as the smallest

conceivable nanocrystal prototypes, Chemical Science 10.1039/D2SC05037D (2022).

- [2] D. Van den Eynden, R. Pokratath, and J. De Roo, Non-aqueous chemistry of group 4 oxo clusters and colloidal metal oxide nanocrystals, *Chemical Reviews* **122**, 10538 (2022).
- [3] U. Schubert, E. Arpac, W. Glaubitt, A. Helmerich, and C. Chau, Primary hydrolysis products of methacrylate-modified titanium and zirconium alkoxides, *Chemistry of Materials* **4**, 291 (1992).
- [4] J. Joo, T. Yu, Y. W. Kim, H. M. Park, F. Wu, J. Z. Zhang, and T. Hyeon, Multigram scale synthesis and characterization of monodisperse tetragonal zirconia nanocrystals, *Journal of the American Chemical Society* **125**, 6553 (2003).
- [5] K. De Keukeleere, S. Coucke, E. De Canck, P. Van Der Voort, F. Delpech, Y. Coppel, Z. Hens, I. Van Driessche, J. S. Owen, and J. De Roo, Stabilization of colloidal ti, zr, and hf oxide nanocrystals by protonated tri-n-octylphosphine oxide (topo) and its decomposition products, *Chemistry of Materials* **29**, 10233 (2017).
- [6] S. Shaw, T. F. Silva, J. M. Bobbitt, F. Naab, C. L. Rodrigues, B. Yuan, J. J. Chang, X. Tian, E. A. Smith, and L. Cademartiri, Building materials from colloidal nanocrystal assemblies: Molecular control of solid/solid interfaces in nanostructured tetragonal zro₂, *Chemistry of Materials* **29**, 7888 (2017).
- [7] S. Gross, Oxocluster-reinforced organic–inorganic hybrid mater.: Effect of transition metal oxoclusters on structural and functional properties, *Journal of Materials Chemistry* **21**, 15853 (2011).
- [8] U. Schubert, Cluster-based inorganic-organic hybrid materials, *Chemical Society Reviews* **40**, 575 (2011).
- [9] J. Moons, F. de Azambuja, J. Mihailovic, K. Kozma, K. Smiljanic, M. Amiri, T. Cirkovic Velickovic, M. Nyman, and T. N. Parac-Vogt, Discrete hf₁₈ metal-oxo cluster as a heterogeneous nanozyme for site-specific proteolysis, *Angew. Chem. Int. Ed.* **59**, 9094 (2020).
- [10] Y. Zhang, F. de Azambuja, and T. N. Parac-Vogt, Zirconium oxo clusters as discrete molecular catalysts for the direct amide bond formation, *Catalysis Science & Technology* **12**, 3190 (2022).
- [11] J.-Y. Huang, H. Xu, E. Peretz, D.-Y. Wu, C. K. Ober, and T. Hanrath, Three-dimensional printing of hierarchical porous architectures, *Chemistry of Materials* **31**, 10017 (2019).
- [12] H. Han, S. Kallakuri, Y. Yao, C. B. Williamson, D. R. Nevers, B. H. Savitzky, R. S. Skye, M. Xu, O. Voznyy, J. Dshemuchadse, L. F. Kourkoutis, S. J. Weinstein, T. Hanrath, and R. D. Robinson, Multiscale hierarchical structures from a nanocluster mesophase, *Nature Materials* **21**, 518 (2022).
- [13] L. Wu, J. Liu, M. Vockenhuber, Y. Ekinici, and S. Castellanios, Hybrid euv resists with mixed organic shells: A simple preparation method, *Eur. J. Inorg. Chem.* **2019**, 4136 (2019).
- [14] S. Kataoka and K. Sue, Enhanced solubility of zirconium oxo clusters from diacetoxyzirconium(iv) oxide aqueous solution as inorganic extreme-ultraviolet photoreists, *European Journal of Inorganic Chemistry* **2022**, e202200050 (2022).
- [15] H. Chang, B. H. Kim, H. Y. Jeong, J. H. Moon, M. Park, K. Shin, S. I. Chae, J. Lee, T. Kang, B. K. Choi, J. Yang, M. S. Bootharaju, H. Song, S. H. An, K. M. Park, J. Y. Oh, H. Lee, M. S. Kim, J. Park, and T. Hyeon, Molecular-level understanding of continuous growth from iron-oxo clusters to iron oxide nanoparticles, *Journal of the American Chemical Society* **141**, 7037 (2019).
- [16] D. C. Gary, M. W. Terban, S. J. L. Billinge, and B. M. Cossairt, Two-step nucleation and growth of inq quantum dots via magic-sized cluster intermediates, *Chemistry of Materials* **27**, 1432 (2015).
- [17] P. H. Willoughby, M. J. Jansma, and T. R. Hoye, A guide to small-molecule structure assignment through computation of (1h and 13c) nmr chemical shifts, *Nature Protocols* **9**, 643 (2014).
- [18] e. a. Giannozzi P., Quantum espresso: a modular and open-source software project for quantum simulations of materials, *Journal of Physics: Condensed Matter* **21**, 695502 (2009).
- [19] e. a. Giannozzi P., Advanced capabilities for materials modelling with quantum espresso, *Journal of Physics: Condensed Matter* **29**, 465901 (2017).
- [20] P. E. Blöchl, Projector augmented-wave method, *Phys. Rev. B* **50**, 17953 (1994).
- [21] M. Ernzerhof and G. E. Scuseria, Assessment of the perdew–burke–ernzerhof exchange-correlation functional, *The Journal of Chemical Physics* **110**, 5029 (1999).